J Incl Phenom Macrocycl Chem (2010) 68:359–367
DOI 10.1007/s10847-010-9795-3

ORIGINAL ARTICLE

Host–guest complexes of the antituberculosis drugs pyrazinamide and isoniazid with cucurbit[7]uril

Nial J. Wheate · Virendra Vora · Nahoum G. Anthony · Fiona J. McInnes

Received: 5 February 2010 / Accepted: 27 April 2010 / Published online: 12 May 2010

Abstract The potential use of cucurbit[7]uril (CB[7]) as an excipient in oral formulations for improved drug physical stability or for improved drug delivery was examined with the antituberculosis drugs pyrazinamide (pyrazine-2-carboxamide) and isoniazid (isonicotinohydrazide). Both drugs form 1:1 host–guest complexes with CB[7] as determined by ^{1}H nuclear magnetic resonance spectrometry, electrospray ionisation mass spectrometry and molecular modelling. Drug binding is stabilised by hydrophobic effects between the pyridine and pyrazine rings of isoniazid and pyrazinamide, respectively, to the inside cavity of the CB[7] macrocycle as well as hydrogen bonds between the hydrazide and amide groups of each drug to the CB[7] carbonyl portals. At pH 1.5, isoniazid binds CB[7] with a binding constant of 5.6×10^{5} M^{-1}, whilst pyrazinamide binds CB[7] at pH 7 with a much smaller binding constant (4.8×10^{3} M^{-1}). Finally, CB[7] prevents drug melting through encapsulation. Where previously pyrazinamide displays a typical melting point of 189 °C and isoniazid 171 °C, by differential scanning calorimetry, no melting or degradation at temperatures up to 280 °C is observed for either drug once bound by CB[7].

Keywords Tuberculosis · Isoniazid · Pyrazinamide · Cucurbituril

N. J. Wheate (✉) · V. Vora · N. G. Anthony · F. J. McInnes
Strathclyde Institute of Pharmacy and Biomedical Sciences, University of Strathclyde, John Arbuthnott Building, 27 Taylor Street, Glasgow G4 0NR, UK
e-mail: nial.wheate@strath.ac.uk

Introduction

Tuberculosis (TB) is a disease caused by the bacterium *Mycobacterium tuberculosis* which results in cough, fever, sweats, fatigue and weight loss, which, if left untreated, eventually leads to death. Despite the availability of a vaccine, each year more than eight million people are infected with TB, of which 1.8 million will die [1]. Treatment of TB is through a course of antibiotics for periods up to 26 weeks. The two main drugs which comprise the most used and effective regimes are pyrazinamide (pyrazine-2-carboxamide) and isoniazid (isonicotinohydrazide) (Fig. 1) [2]. Pyrazinamide is principally active against semidormant or dormant bacteria within macrophages or the acidic environment of caseous foci whilst isoniazid is effective against all rapidly dividing forms of the bacterium [2]. The development of multidrug resistant TB, however, drives the need for new drugs [3–7] and better drug delivery to combat the disease [8, 9]. This includes the development of targeted delivery mechanisms for antibiotics that are able to recognise, and bind to TB bacteria and thus increase the selectivity, uptake and effectiveness of the drug. Such delivery may decrease the chance of the bacteria developing antibiotic resistance through improved kill rates over shorter treatment times.

Cucurbit[7]uril (CB[7], see Fig. 1) is one compound in a family of glycoluril-based macrocycles [10, 11]. With its hydrophobic cavity and hydrophilic portals, CB[7] is capable of forming a range of host–guest complexes with organic and inorganic compounds. Cucurbit[7]uril is largely non-toxic in vitro and in vivo [12], it has good water solubility compared with other CB[*n*]s and an ideal cavity size for drug storage and release, which means it has enormous potential as a drug delivery vehicle [13–38], a

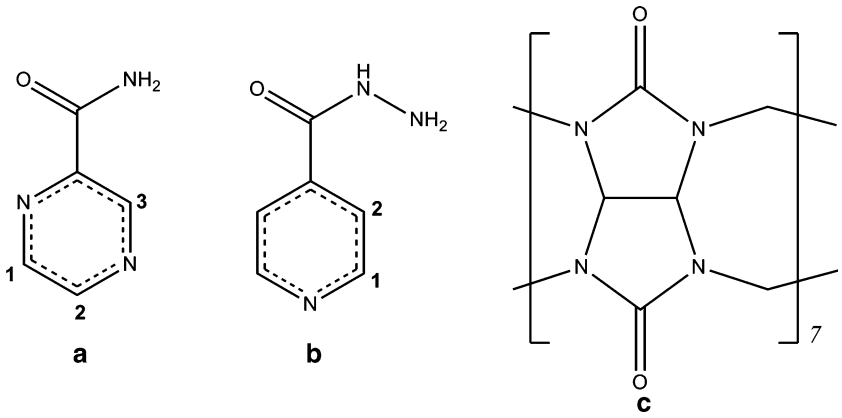

Fig. 1 The chemical structures of **a** pyrazinamide, **b** isoniazid and **c** cucurbit[7]uril (CB[7]) showing the numbering scheme used for ^{1}H NMR

biodiagnostic agent [39–46] and in modulating bioregulation and function [47–51].

Partial or full encapsulation by CB[7] can have a number of effects on a drug, including: providing physical stability against degradation and changes of solid state phase during manufacturing, formulation and storage [14, 15]; prevention of in vivo detoxification/degradation and reduction of drug side-effects [16]; modulating cellular drug uptake [52], and targeted delivery [53]. In addition, further delivery enhancements are possible and include: taste masking, and altered drug absorption and biodistribution profiles.

In this paper we report the characterisation of the host–guest complexes of pyrazinamide and isoniazid with cucurbit[7]uril by ^{1}H nuclear magnetic resonance spectroscopy, electrospray ionisation mass spectrometry, molecular modelling, fluorescent guest displacement assays and differential scanning calorimetry. The results are discussed in the context of improving drug manufacture, storage and delivery.

Results and discussion

^{1}H Nuclear magnetic resonance spectroscopy

One of the most powerful techniques for examining drug-CB[7] host–guest complexes is ^{1}H NMR spectroscopy. Typically, drug proton resonances located within the cavity of CB[7] exhibit a significant upfield (lower ppm) shift due to shielding, whilst drug protons located outside, but close to, the CB[7] portals shift slightly downfield (higher ppm) due to a deshielding effect [54]. These changes in chemical shift of the drug resonances, together with changes in line width, give information on the location, orientation and the kinetics of the binding of a drug bound to CB[7].

Free pyrazinamide has three peaks in the aromatic region at 9.15 (H3), 8.78 (H2) and 8.71 ppm (H1) in D_2O (Fig. 2). Upon the addition of one equivalent of CB[7], all three drug resonances shift upfield to 9.06, 8.69 and 8.55 ppm, respectively. The larger upfield shift of the H1 resonance ($\Delta = 0.16$ ppm) compared with the H2 and H3 resonances ($\Delta = 0.08/0.09$ ppm) indicates that the H1 proton is located deeper within the cavity of CB[7] than H2 or H3. The addition of excess CB[7] results in a further upfield shift of the pyrazinamide drug resonances to 8.96, 8.58 and 8.38 ppm (see Fig. 2), giving a final change in chemical shift of 0.19 ppm for the H2 and H3 protons and 0.33 ppm for the H1 proton. The pyrazinamide drug resonances are also considerably broadened upon binding by CB[7] and given that only one set of drug peaks is seen at all drug to CB[7] ratios we conclude that the binding kinetics, on the ^{1}H NMR timescale, are in fast exchange between free drug and bound drug. The continual upfield shift of the drug resonances upon increasing CB[7] also indicates that encapsulation of the drug is a dynamic process in equilibrium between the free and bound forms. As CB[7] is added to the solution the equilibrium shifts further towards the host–guest complex.

Free isoniazid has just two non-exchangeable proton resonances in D_2O at 8.64 ppm for the H1 proton and 7.67 ppm for H2 (Fig. 3). Upon addition of one equivalent of CB[7] the resonances move upfield to 8.47 ($\Delta = 0.17$) and 7.48 ppm ($\Delta = 0.19$), respectively. The addition of excess CB[7] shifts the drug resonances further to 8.39 and 7.42 ppm, respectively. As observed for pyrazinamide, the resonances for isoniazid broadened significantly upon binding of CB[7], and again, as only one set of drug peaks is seen at all drug to CB[7] ratios we conclude that the binding kinetics, on the ^{1}H NMR timescale, are in fast exchange. Similar to pyrazinamide, the results also indicate that binding is in equilibrium between the free and bound forms, which shifts more towards the bound form as CB[7] is added.

When bound to both pyrazinamide and isoniazid, CB[7] has three resonances in the ^{1}H NMR spectra at 5.72, 5.47 and 4.17 ppm, which do not significantly change chemical shift upon the addition of either drug, as is usually the case

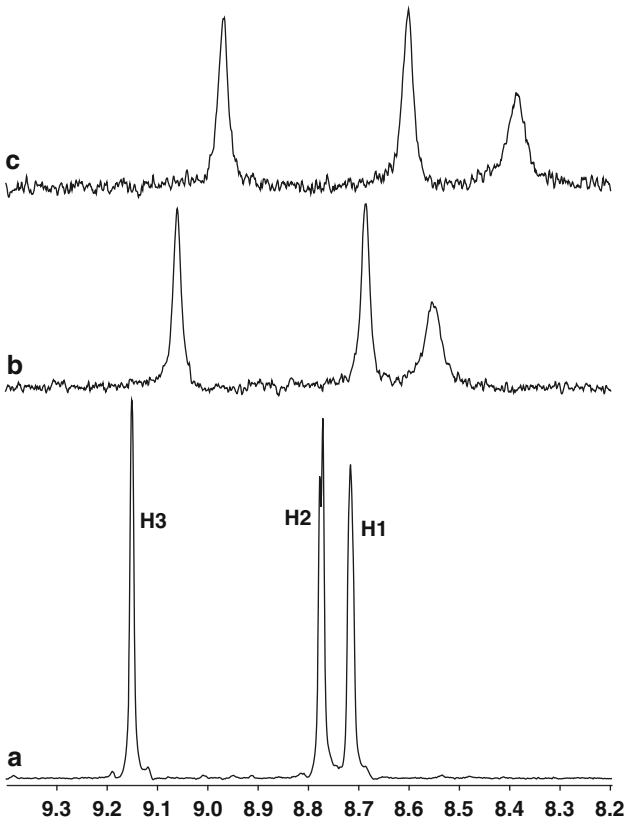

Fig. 2 The ^{1}H NMR spectra (D_2O, 400 MHz, ~pH 7) of **a** free pyrazinamide **b** with 1 equivalent of CB[7] and **c** with excess CB[7], showing the upfield shift and line broadening of the drug resonances upon binding by the macrocycle. The proton numbers, based on the assignments in Fig. 1, are shown

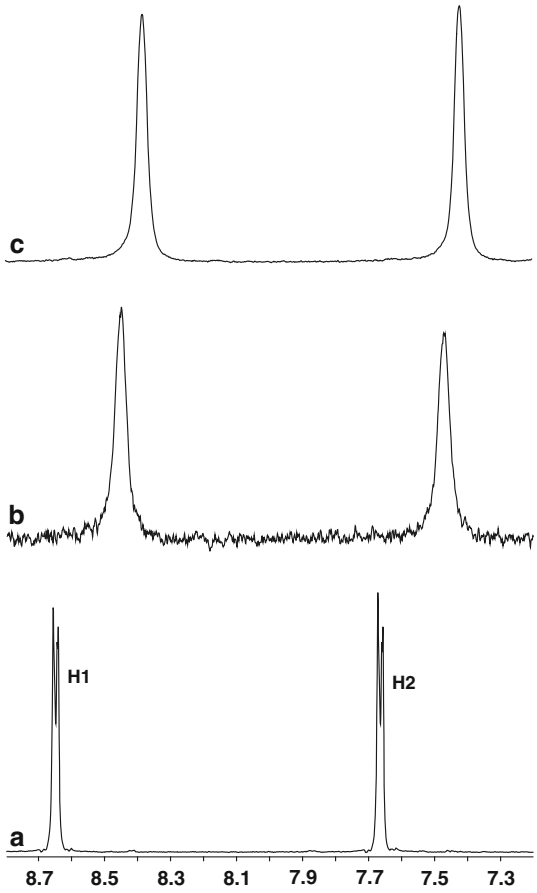

Fig. 3 The ^{1}H NMR spectra (D_2O, 400 MHz, ~pH 7) of **a** free isoniazid **b** with 1 equivalent of CB[7] and **c** with excess CB[7], showing the upfield shift and line broadening of the drug resonances upon binding by the macrocycle. The proton numbers, based on the assignments in Fig. 1, are shown

as all CB[7] protons are exocyclic; pointing away from the CB[7] cavity [54].

The formation of the host–guest complexes of pyrazinamide and isoniazid were also examined by ^{1}H NMR at low pH. At a pH of 1 the pyrazinamide resonances occur at 9.14, 8.77 and 8.71 ppm. When a large excess of CB[7] is added all three peaks shift upfield to 9.01 ($\Delta = -0.13$), 8.66 ($\Delta = -0.11$) and 8.50 ppm ($\Delta = 0.21$ ppm). Similarly, at pH 1 the two resonances of isoniazid occur at 8.95 and 8.35 ppm. Addition of a large excess of CB[7] moves the resonances to 8.47 ($\Delta = -0.48$) and 7.34 ppm ($\Delta = -1.01$ ppm), respectively, which are considerably larger than the shifts observed at neutral pH. These results indicate that both drugs form host–guest complexes with CB[7] in strongly acidic solutions.

Electrospray ionisation mass spectrometry

Mass spectrometry was used to further confirm the formation of host–guest complexes of pyrazinamide and isoniazid with CB[7]. In the spectrum of pyrazinamide with CB[7], five peaks of interest are observed (Fig. 4); three which represent free CB[7] at 593.5, 1185.6 and 1202.4 m/z, with $[H^+$ and $Na^+]^{2+}$, 1 Na^+ and 1 K^+ ions, respectively. Two host–guest complex peaks are observed at 654.9 and 665.80 m/z. These represent CB[7]-drug complexes with a 2^+ charge, coming from their formation with either one H^+ and one Na^+ or with two Na^+ ions, respectively.

For isoniazid, seven assignable peaks are observed in the spectrum (see Fig. 4). Free CB[7] is observed at 1163.3 and 1185.6 m/z, respectively. Free isoniazid is observed as the acid salt at 138.1 m/z with CB[7]-drug host–guest complex peaks observed at 651.1, 662.0, 672.9 and 1300.4 m/z. The first three peaks represent host–guest complexes with a 2 + charge whilst the peak at 1300 m/z is a 1+ complex with a single H^+ ion.

Molecular modelling

Molecular models of the host–guest complexes of pyrazinamide and isoniazid with CB[7] were generated using

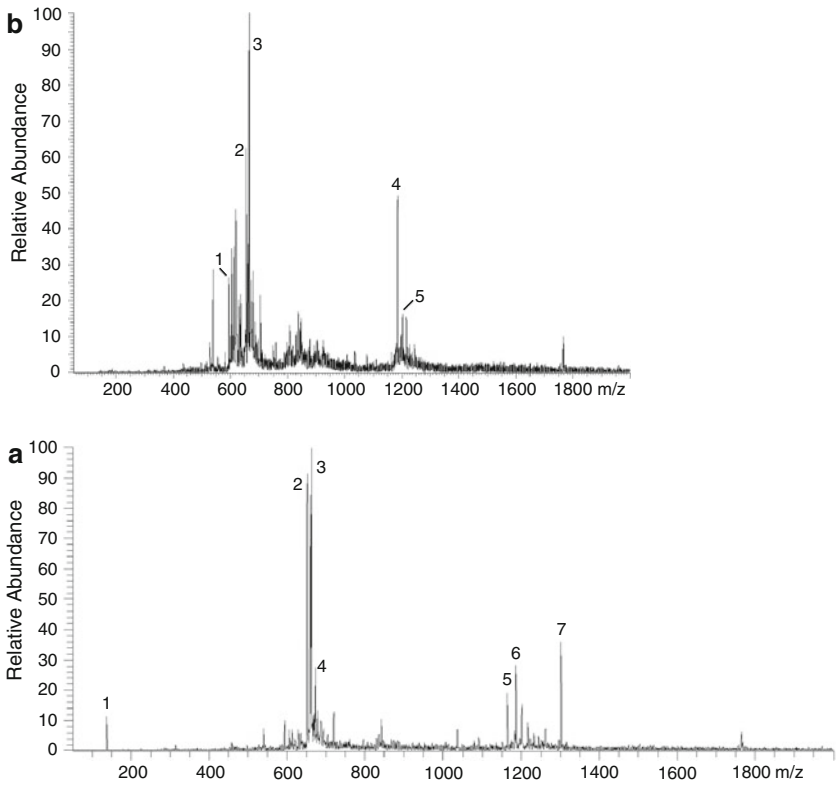

Fig. 4 The electrospray ionisation mass spectra (positive mode, ~pH 7) of **a** isoniazid showing free drug (peak 1), free CB[7] (peaks 5 and 6) and the 1:1 host–guest complex (peaks 2, 3, 4 and 7); and **b** pyrazinamide showing free CB[7] (peaks 1, 4 and 5) and the 1:1 host–guest complex (peaks 2 and 3)

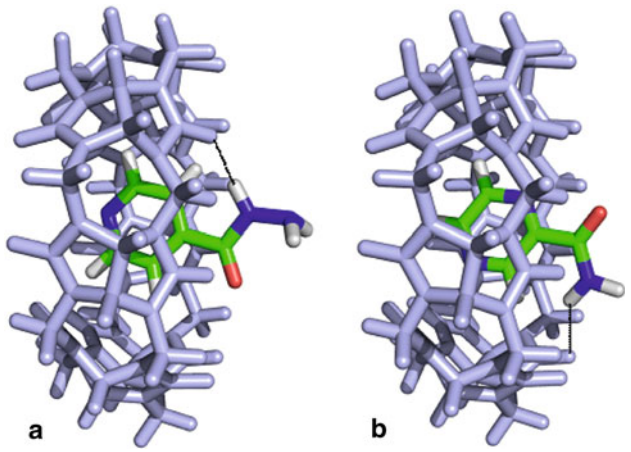

Fig. 5 Minimised host–guest structures of **a** isoniazid and **b** pyrazinamide with CB[7]. Intermolecular hydrogen bonds are shown as *dotted lines*

Insight II and CDiscover (Accelrys Inc., San Diego, USA). The molecular model of pyrazinamide and CB[7] shows a 1:1 host–guest complex with the pyrazine ring located in the cavity of CB[7], where binding is stabilised by hydrophobic interactions (Fig. 5a). Binding is further stabilised by a single hydrogen bond between the drug's amide group and a single CB[7] carbonyl oxygen (NH–O; 2.31 Å). Whilst the amide NH of pyrazinamide may be hydrogen bonded to the CB[7] portal there could also be an interaction with the solvent instead; however, in this study we examined direct interactions between the drug and CB[7] only and direct hydrogen bonding of the drug with the solvent will not be observed using our an implicit solvation model. The molecular model is consistent with the ^{1}H NMR data in that the H1 proton of the drug is approximately in the centre of the CB[7] cavity, hence its large upfield shift in the NMR spectra, whilst the H2 and H3 protons are located closer to the portals, which is why they shift upfield to a lesser extent compared with the H1 proton.

A similar 1:1 host–guest complex is observed for the molecular model of isoniazid and CB[7] (Fig. 5b). The pyridine ring is located within the CB[7] cavity with the hydrazine NH group forming a hydrogen bond to a single CB[7] carbonyl oxygen (NH–O; 2.45 Å).

Determination of binding constants

A fluorescent guest displacement assay was used in an attempt to determine the binding constants of pyrazinamide and isoniazid. This assay is based on 2-aminoanthracene (2-AAH) and at a pH of 1.5, with the results analysed using the following equation [55, 56]:

$$K_{2AAH}[2AAH] = K_C[Drug]$$

where K_{2AAH} is the binding constant of 2-AAH to CB[7] (8.0×10^5 M^{-1}) [43], [2AAH] is the fixed concentration of 2-AAH (and CB[7]), K_C is the binding constant to CB[7]

and [Drug] is the concentration of drug that gives a 50% increase in fluorescence at 508 nm. As both drugs are administered as oral tablets, the pH used in this experiment is indicative of the in vivo stomach environment upon tablet disintegration [2].

Titration of isoniazid into a fixed concentration of 2-aminoanthracence (5 μM) and CB[7] (5 μM) results in a progressive change of the fluorescence spectrum between 380 and 600 nm. The two large, sharp peaks at 390 and 411 nm decrease in intensity whilst the broad peak at 508 nm increases in intensity, as the 2-aminoanthracene is displaced from the CB[7] cavity with the increasing concentration of isoniazid (Fig. 6). A binding curve for the drug was generated from a plot of the fluorescence intensity at 508 nm as a function of isoniazid concentration (Inset Fig. 6). From this binding curve the 50% fluorescence enhancement point was calculated and used to determine a binding constant of 5.6×10^5 M^{-1}. This high binding constant may be a function of the increased charge of isoniazid at this pH. The drug has three ionisable groups with the following pKa values: pyridine nitrogen, 1.8; hydrazine –NH group, 3.5; and the hydrazine $–NH_2$ group, 10.8 [57]. At this pH, the charge on the drug is 2+ or 3+ which may help stabilise the host–guest complex with additional ion–dipole interactions, compared with the drug at pH 7 when it has only a single positive charge.

Unlike isoniazid, upon titration of pyrazinamide into the 2-aminoanthracene and CB[7] solution there was no change in the fluorescence spectra at concentrations of up to 1 mM of added pyrazinamide. Pyrazinamide has just one ionisable group, the amine, which has a pKa of 0.5, and is therefore uncharged at pH 1 [58]. As the ^{1}H NMR results indicated that isoniazid forms a host–guest complex with CB[7] at low pH the fluorescence results therefore indicate that binding to CB[7] is not strong enough to displace the 2-aminoanthracene.

The binding constant at pH 7 was therefore determined using a methylene blue displacement assay instead [59]. The fluorescence of methylene blue increases from 60 to 380 upon the addition of CB[7], and with a hypsochromic shift from 675 to 670 nm. Addition of pyrazinamide reduces the fluorescence intensity, but only upon the addition of large concentrations of drug (up to 300 μM). From this a binding constant of 4.8×10^3 M^{-1} can be calculated.

Differential scanning calorimetry

Pyrazinamide is known to crystallise as one of four polymorphs: α-, β-, γ-, δ-pyrazinamide, which are formed when different temperatures and solvents are used for their synthesis [58, 60–62]. The different polymorphs are structurally related, with all types stabilised by NH–O, NH–N and unusual CH–N "hydrogen" bonds. Because these polymorphs are so similar it is possible that they may interconvert during drug manufacture or storage, which may affect their solubility and uptake. In contrast, isoniazid is not known to form polymorphs with only a single crystal structure reported to date [63, 64].

The effect of CB[7] on the melting of pyrazinamide and isoniazid was examined using differential scanning calorimetry (Fig. 7). Although pyrazinamide has been in use for a long time no DSC data for the drug is available in the literature. Under the experimental conditions used, pyrazinamide shows a single endotherm peak at 189.1 °C, consistent with the stated melting point of all four crystal types of pyrazinamide. The enthalpy of fusion from this melting peak was found to be 27.28 kJ mol^{-1}.

The physical stability of isoniazid has previously been examined by Rastogi et al. [65] who reported a single sharp endotherm melting peak for the drug at 175 °C. Our result is similar although at a slightly lower temperature of 170.6 °C and with an enthalpy of fusion of 31.7 kJ mol^{-1}.

Freeze dried samples of each drug with one equivalent of CB[7] demonstrate that the macrocycle completely prevents drug melting as the usual drug crystal lattice does

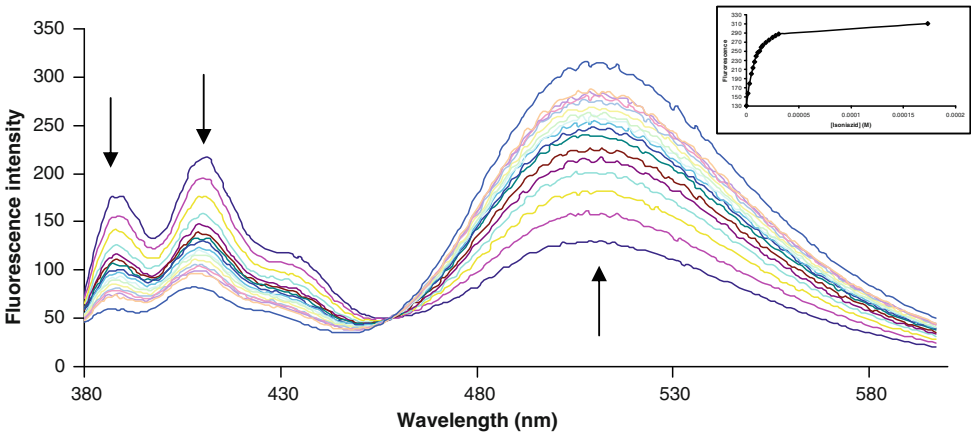

Fig. 6 The fluorescence spectra (Ex: 374 nm) of 2-aminoanthracene (5 μM) at pH 1.5, in the presence of 1 mol equivalent of CB[7] and with increasing isoniazid concentration. The *arrows* indicate the direction of change. *Inset*: A plot of fluorescence intensity, at a wavelength of 508 nm, as a function of isoniazid concentration

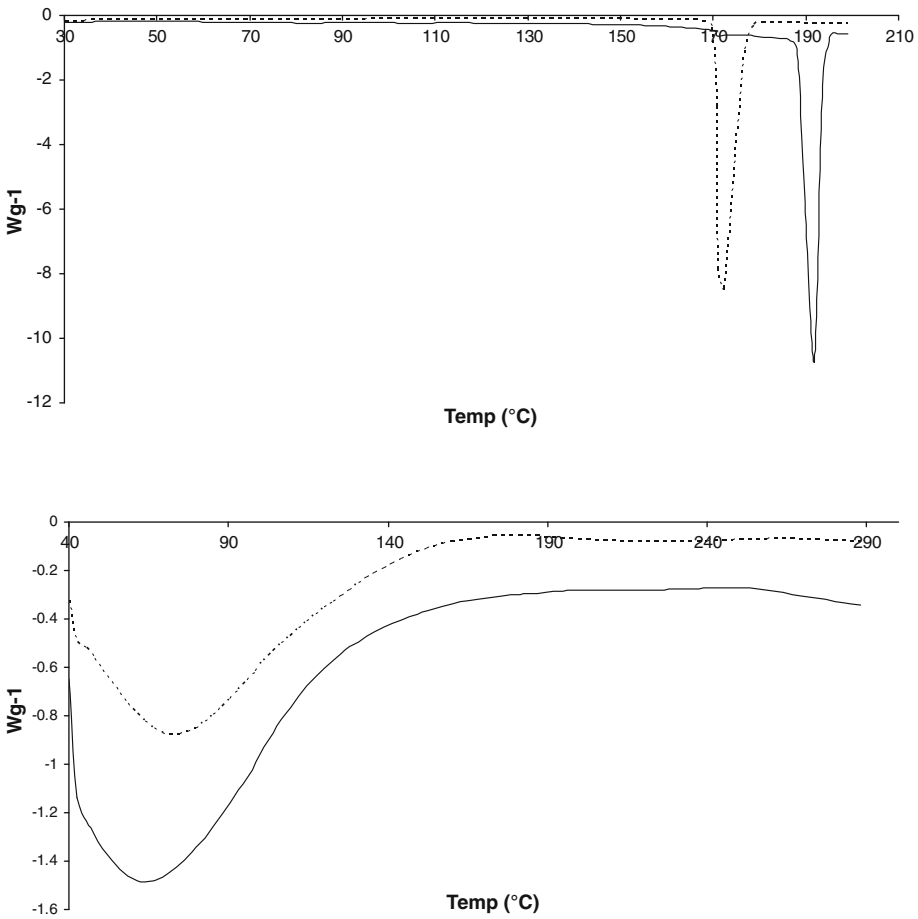

Fig. 7 The differential scanning calorimetry spectra of (*top*) the free drugs pyrazinamide (—) and isoniazid (- - -), and (*bottom*) the host–guest complexes of pyrazinamide (—) and isoniazid (- - -) with CB[7]

not exist because each drug is encapsulated within the CB[7] cavity (see Fig. 7). Neither drug melts below 280 °C with only a broad peak observed between 40 and 150 °C, which we assign as the loss of waters of crystallisation from the host–guest complex. This is typical of the high hydration state that many host–guest complexes of CB[*n*]s form and has been observed for other host–guest complexes [18, 66]. As pyrazinamide and isoniazid have both been shown to be resistant to chemical degradation [67], the effect of CB[7] to prevent this was not examined in this study. These results indicate that CB[7] may be used to prevent interconversion of drug crystal polymorphs to ensure a consistent drug form is produced and maintained during manufacture and storage.

Conclusions

The antibiotic treatment of TB can be greatly improved through the development of targeted delivery mechanisms for antibiotics that are able to recognise, and bind to TB bacteria and thus increase the selectivity, uptake and effectiveness of the drug. Such delivery may decrease the chance of the bacteria developing antibiotic resistance through improved kill rates over shorter treatment times. In this work we have investigated the encapsulation of the drugs pyrazinamide and isoniazid in CB[7] as a first step in the development of targeted delivery methods. Using ^{1}H NMR, ESI–MS and molecular modelling we have shown that CB[7] forms host–guest complexes with the antituberculosis drugs pyrazinamide and isoniazid. At an in vivo relevant pH, isoniazid binding to CB[7] is strong with a K_b in the order of 10^5 M^{-1}, whilst pyrazinamide appears to bind only very weakly (10^3 M^{-1}). Differential scanning calorimetry demonstrates that CB[7] imparts significant physical stability to both drugs. The results of this work therefore indicate that CB[7] may have two potential biomedical applications. First, as pyrazinamide can be grown in four distinct crystal types which may interconvert, or change to an amorphous product during manufacture, where high temperatures and variable humidity are used [68], then CB[7] could potentially be used to stabilise the drug during manufacture or storage against changes in physical form. In such a case, the pyrazinamide-CB[7] host–guest complex would be stable until swallowed, at which point the low pH in the stomach would cause the CB[7] to release the drug, thus ensuring no change to the drug's biodistribution, uptake or mode of action.

Alternatively, the results obtained in this work for isoniazid demonstrate the potential, and provides the basis for the development of, CB[7] as a drug delivery vehicle for active targeting of TB. Functionalised CB[7] are known in the literature, and subsequent attachment of TB targeting groups, such as aptamers or monoclonal antibodies, may allow CB[7] to deliver isoniazid more effectively to the bacterium.

Experimental

Materials

Isoniazid and D_2O (99.9%) were purchased from Sigma–Aldrich. CB[7] was made as previously described [69]. Pyrazinamide was purchased from Sigma–Aldrich, but was purified before use from a slowly evaporated solution of 50% ethanol/50% water.

^{1}H nuclear magnetic resonance

Stock solutions of CB[7] were made in D_2O to a concentration of 2 mM. Stocks of each drug (20 mM) were prepared in D_2O. Aliquots of CB[7] and drug were combined and made up to 600 μL to yield various CB[7] to drug ratios with final concentrations between 0.5 and 1.5 mM. Samples at pH 1 were made by the addition of DCl. ^{1}H NMR spectra were then recorded on a JEOL JNM-LA400 spectrometer. Spectra were obtained using between 16-128 scans, with a d1 of 2 s and a spectral width of 5,000 Hz. Spectra were referenced internally to the solvent peak (HDO: 4.78 ppm @ 25 °C).

Electrospray ionisation mass spectrometry

Positive ion electrospray ionisation (ESI) mass spectra were recorded on a Finnigan LTQ Orbitrap. Samples were dissolved in H_2O to a concentration of 500 μM then 40 μL was diluted to 1 mL with a 50% methanol/50% 0.1 formic acid solution and injected into the instrument at a flow rate of 400 μL min^{-1}. The capillary temperature and voltage were 230 °C and 40 V, respectively, with a source voltage of 4,500 V.

Molecular modelling

Insight II and CDiscover software (Accelrys Inc., San Diego, CA) were used to perform all calculations and molecule handling employing the cff force field (for both atom typing and charges) [70]. All simulations were performed using a dual processor Hewlett-Packard 3.2 GHz xw8200 workstation. The starting CB[7] structure was obtained from a single-crystal X-ray structure [66], and the drugs pyrazinamide and isoniazid manually docked, placing the drug in a region corresponding to a high shielding of its protons, as determined by ^{1}H NMR experiments. Water was not explicitly included in the modelling calculation, but implicit solvation was granted by the use of a dielectric constant [71]. The systems were then allowed to minimise *in vacuo* without restraints using a distant-dependent dielectric constant of 4 r_{ij} until a derivative of 0.01 kcal mol^{-1} Å^{-2} was achieved [72].

Determination of binding constants

CB[7] and 2-AAH were dissolved in water (3.000 mL) which had previously been adjusted to pH 1.5 by the addition of HCl. Fluorescence intensity was determined on a Varian Cary Eclipse spectrophotometer in a 1 cm quartz cell, using an excitation wavelength of 374 nm [43], with a medium scan speed between 380 and 600 nm. Alternatively, CB[7] and methylene blue were dissolved in water (3.000 mL) to a concentration of 6 μM and the fluorescence intensity measured between 625 and 800 nm using an excitation wavelength of 620 nm [59]. Pyrazinamide and isoniazid (2.5 mM) were then titrated into the solutions in 2, 4 or 40 μL increments, with mixing of the solutions for 1 min before fluorescence was measured. Binding constants were determined based on previous fluorescence displacement assays using ethidium bromide [55, 56].

Differential scanning calorimetry

Experiments were conducted using a Mettler Toledo DSC 8222e. Each sample (approximately 2–10 mg), was prepared by freeze drying a 1:1 CB[7] to drug solution from water, which was then weighed in an alumina or sealed aluminium pan. Samples were then heated at a rate of 10 °C min^{-1} at temperatures up to 290 °C.

References

1. Cole, S.T., Eisenach, K.D., McMurray, D.N., Jacobs, W.R. Jr. (eds.): Tuberculosis and the tubercle bacillus. ASM Press, Washington (2005)
2. American thoracic society/Centers for disease control and prevention/Infectious diseases society of America: treatment of tuberculosis. Am. J. Respir. Crit. Care Med. **167**, 603–662 (2003)
3. Mugnaini, C., Pasquini, S., Corelli, F.: The 4-quinolone-3-carboxylic acid motif as a multivalent scaffold in medicinal chemistry. Curr. Med. Chem. **16**, 1746–1767 (2009)
4. Manetti, F., Magnani, M., Castagnolo, D., Passalacqua, L., Botta, M., Corelli, F., Saddi, M., Deidda, D., De Logu, A.: Ligand-based virtual screening, parallel solution-phase and microwave-assisted synthesis as tools to identify and synthesize new inhibitors of Mycobacterium tuberculosis. ChemMedChem **1**, 973–989 (2006)

5. Chhabria, M., Jani, M.H.: Design, synthesis and antimycobacterial activity of some novel imidazo[1, 2-c]pyrimidines. Eur. J. Med. Chem. **44**, 3837–3844 (2009)
6. Chhabria, M., Jani, M., Patel, S.: New frontiers in the therapy of tuberculosis: fighting with the global menace. Mini. Rev. Med. Chem. **9**, 401–430 (2009)
7. Rogoza, L.N., Salakhutdinov, N.F., Tolstikov, G.A.: Natural and synthetic compounds with an antimycobacterial activity. Mini. Rev. Org. Chem. **6**, 135–151 (2009)
8. Mendez, M.P., Landon, M.E., McCloud, M.K., Davidson, P., Christensen, P.J.: Co-infection with pansensitive and multidrug-resistant strains of *Mycobacterium tuberculosis*. Emerg. Infect. Dis. **15**, 578–580 (2009)
9. Mathema, B., Kurepina, N.E., Bifani, P.J., Kreiswirth, B.N.: Molecular epidemiology of tuberculosis: current insights. Clin. Microbiol. Rev. **19**, 658–685 (2006)
10. Isaacs, L.: Cucurbit[*n*]urils: from mechanism to structure and function. Chem. Commun. 619–629 (2009)
11. Kim, K., Selvapalam, N., Ko, Y.H., Park, K.M., Kim, D., Kim, J.: Functionalized cucurbiturils and their applications. Chem. Soc. Rev. **36**, 267–279 (2007)
12. Uzunova, V.D., Cullinane, C., Brix, K., Nau, W.M., Day, A.I.: Toxicity of cucurbit[7]uril and cucurbit[8]uril: an exploratory in vitro and in vivo study. Org. Biomol. Chem. **8**, 2037–2042 (2010)
13. Walker, S., Kaur, R., McInnes, F.J., Wheate, N.J.: Oral drug formulations. Great Britian Patent Application No. 0906003.9, April 2009, 24 pp
14. McInnes, F.J., Anthony, N.G., Kennedy, A.R., Wheate, N.J.: Solid state stabilisation of the orally delivered drugs atenolol, glibenclamide, memantine and paracetamol through their complexation with cucurbit[7]uril. Org. Biomol. Chem. **8**, 765–773 (2010)
15. Kennedy, A.R., Florence, A.F., McInnes, F.J., Wheate, N.J.: A chemical preformulation study of a host-guest complex of cucurbit[7]uril and a multinuclear platinum agent for enhanced anticancer drug delivery. Dalton Trans. 7695–7700 (2009)
16. Wheate, N.J.: Improving platinum(II)-based anticancer drug delivery using cucurbit[*n*]urils. J. Inorg. Biochem. **102**, 2060–2066 (2008)
17. Wheate, N.J., Taleb, R.I., Krause-Heuer, A.M., Cook, R.L., Wang, S., Higgins, V.J., Aldrich-Wright, J.R.: Novel platinum(II)-based anticancer complexes and molecular hosts as their drug delivery vehicles. Dalton Trans. 5055–5064 (2007)
18. Kemp, S., Wheate, N.J., Wang, S., Collins, J.G., Ralph, S.F., Day, A.I., Higgins, V.J., Aldrich-Wright, J.R.: Encapsulation of platinum(II)-based DNA intercalators within cucurbit[6, 7, 8]urils. J. Biol. Inorg. Chem. **12**, 969–979 (2007)
19. Kemp, S., Wheate, N.J., Stootman, F.H., Aldrich-Wright, J.R.: The host-guest chemistry of proflavine with cucurbit[6, 7, 8]urils. Supramol. Chem. **19**, 475–484 (2007)
20. Wheate, N.J., Buck, D.P., Day, A.I., Collins, J.G.: Cucurbit[*n*]uril binding of platinum anticancer complexes. Dalton Trans. 451–458 (2006)
21. Wheate, N.J., Day, A.I., Blanch, R.J., Arnold, A.P., Cullinane, C., Collins, J.G.: Multi-nuclear platinum complexes encapsulated in cucurbit[*n*]uril as an approach to reduce toxicity in cancer treatment. Chem. Commun. 1424–1425 (2004)
22. Zhao, Y., Bali, M.S., Cullinane, C., Day, A.I., Collins, J.G.: Synthesis, cytotoxicity and cucurbituril binding of triamine linked dinuclear platinum complexes. Dalton Trans. 5190–5198 (2009)
23. Buck, D.P., Abeysinghe, P.M., Cullinane, C., Day, A.I., Collins, J.G., Harding, M.M.: Inclusion complexes of the antitumour metallocenes Cp_2MCl_2 (M = Mo, Ti) with cucurbit[n]urils. Dalton Trans. 2328–2334 (2008)
24. Bali, M.S., Buck, D.P., Coe, A.J., Day, A.I., Collins, J.G.: Cucurbituril binding of trans-$[\{PtCl(NH_3)_2\}_2(\mu\text{-}NH_2(CH_2)_8NH_2)]^{2+}$ and the effect on the reaction with cysteine. Dalton Trans. 5337–5344 (2006)
25. Wang, R., Bardelang, D., Waite, M., Udachin, K.A., Leek, D.M., Yu, K., Ratcliffe, C.I., Ripmesster, J.A.: Inclusion complexes of coumarin in cucurbiturils. Org. Biomol. Chem. **7**, 2435–2439 (2009)
26. Jeon, Y.J., Kim, S.-Y., Ko, Y.H., Sakamoto, S., Yamaguchi, K., Kim, K.: Novel molecular drug carrier: Encapsulation of oxaliplatin in cucurbit[7]uril and its effects on stability and reactivity of the drug. Org. Biomol. Chem. **3**, 2122–2125 (2005)
27. Choi, J., Kim, J., Kim, K., Yang, S.-T., Kim, J.-I., Jon, S.: A rationally designed macrocyclic cavitand that kills bacteria with high efficacy and good selectivity. Chem. Commun. 1151–1153 (2007)
28. Saleh, N.I., Koner, A.L., Nau, W.M.: Activation and stabilization of drugs by supramolecular pKa shifts: drug-delivery applications tailored for cucurbiturils. Angew. Chem. Int. Ed. **47**, 5398–5401 (2008)
29. Lim, Y.-b., Kim, T., Lee, J.W., Kim, S.-M., Kim, H.-J., Kim, K., Park, J.-S.: Self-assembled ternary complex of cationic dendrimer, cucurbituril, and DNA: noncovalent strategy in developing a gene delivery carrier. Bioconjug. Chem. **13**, 1181–1185 (2002)
30. Wang, R., Wyman, I.W., Wang, S., Macartney, D.H.: Encapsulation of a b-carboline in cucurbit[7]uril. J. Incl. Phenom. Macrocycl. Chem. **64**, 233–237 (2009)
31. Park, K.M., Suh, K., Jung, H., Lee, D.-W., Ahn, Y., Kim, J., Baek, K., Kim, K.: Cucurbituril-based nanoparticles: a new efficient vehicle for targeted intracellular delivery of hydrophobic drugs. Chem. Commun. 71–73 (2009)
32. Angelos, S., Yang, Y.-W., Patel, K., Stoddart, J.F., Zink, J.I.: pH-responsive supramolecular nanovalves based on cucurbit[6]uril pseudorotaxanes. Angew. Chem. Int. Ed. **47**, 2222–2226 (2008)
33. Wang, R., Macartney, D.H.: Cucurbit[7]uril host-guest complexes of the histamine H_2-receptor antagonist ranitine. Org. Biomol. Chem. **6**, 1955–1960 (2008)
34. Lee, H.K., Park, K.M., Jeon, Y.J., Kim, D., Oh, D.H., Kim, H.S., Park, C.K., Kim, K.: Vesicle formed by amphiphilc cucurbit[6]uril: versatile, noncovalent modification of the vesicle surface, and multivalent binding of sugar-decorated vesicles to lectin. J. Am. Chem. Soc. **127**, 5006–5007 (2005)
35. Kim, J., Ahn, Y., Park, K.M., Kim, Y., Ko, Y.H., Oh, D.H., Kim, K.: Carbohydrate wheels: cucurbituril-based carbohydrate clusters. Angew. Chem. Int. Ed. **46**, 7393–7395 (2007)
36. Zhao, Y., Buck, D.P., Morris, D.L., Pourgholami, M.H., Day, A.I., Collins, J.G.: Solubilisation and cytotoxicity of albendazole encapsulated in cucurbit[*n*]uril. Org. Biomol. Chem. **6**, 4509–4515 (2008)
37. Huang, X., Tan, Y., Zhou, Q., Wang, Y.: Fabrication of cucurbit[6]uril mediated alginate physical hydrogel beads and their application as drug carriers. e-polymers **95**, 1–11 (2008)
38. Angelos, S., Khashab, N.M., Yang, Y.-W., Trabolsi, A., Khatib, H.A., Stoddart, J.F., Zink, J.I.: pH clock-operated mechanized nanoparticles. J. Am. Chem. Soc. **131**, 12912–12914 (2009)
39. Kim, B.S., Ko, Y.H., Kim, Y., Lee, H.J., Selvapalam, N., Lee, H.C., Kim, K.: Water soluble cucurbit[6]uril derivative as a potential Xe carrier for ^{129}Xe NMR-based biosensors. Chem. Commun. 2756–2758 (2008)
40. Rekharsky, M.V., Yamamura, H., Ko, Y.H., Selvapalam, N., Kim, K., Inoue, Y.: Sequence recognition and self-sorting of a dipeptide by cucurbit[6]uril and cucurbit[7]uril. Chem. Commun. 2236–2238 (2008)
41. Rankin, M.A., Wagner, B.D.: Fluorescence enhancement of curcumin upon inclusion into cucurbituril. Supramol. Chem. **16**, 513–519 (2004)

42. Li, C., Li, J., Jia, X.: Selective binding and highly sensitive fluorescent sensor of palmatine and dehydrocorydaline alkaloids by cucurbit[7]uril. Org. Biomol. Chem. **7**, 2699–2703 (2009)
43. Wang, R., Yuan, L., Macartney, D. H.: A green to blue fluorescence switch of protonated 2-aminoanthracene upon inclusion in cucurbit[7]uril. Chem. Commun. 5867–5869 (2005)
44. Bailey, D.M., Hennig, A., Uzunova, V.D., Nau, W.M.: Supramolecular tandem enzyme assays for multiparameter sensor arrays and enantiomeric excess determination of amino acids. Chem.—Eur J. **14**, 6069–6077 (2008)
45. Hennig, A., Bakirci, H., Nau, W.M.: Label-free continuous enzyme assays with macrocycle-fluorescent dye complexes. Nat. Methods **4**, 629–632 (2007)
46. Nau, W.M., Ghale, G., Hennig, A., Bakirci, H., Bailey, D.M.: Substrate-selective supramolecular tandem assays: monitoring enzyme inhibition of arginase and diamine oxidase by fluorescent dye displacement from calixarene and cucurbituril macrocycles. J. Am. Chem. Soc. **131**, 11558–11570 (2009)
47. Huo, F.-J., Yin, C.-X., Yang, P.: The crystal structure, self-assembly, DNA-binding and cleavage studies of the [2]pseudorotaxane composed of cucurbit[6]uril. Bioorg. Med. Chem. Lett. **17**, 932–936 (2007)
48. Isobe, H., Sato, S., Lee, J.W., Kim, H.-J., Kim, K., Nakamura, E.: Supramolecular modulation of action of polyamine on enzyme/DNA interactions. Chem. Commun. 1549–1551 (2005)
49. Ke, C.-F., Zhhang, H.-Y., Liu, Y., Feng, X.-Z.: Controllable DNA condensation through cucurbit[6]uril in 2D pseudopolyrotaxanes. Chem. Commun. 3374–3376 (2007)
50. Wang, R., MacGillivray, B.C., Macartney, D. H.: Stabilization of the base-off forms of vitamin B12 and coenzyme B12 by encapsulation of the a-axial 5,6-dimethylbenzimidazole ligand with cucurbit[7]uril. Dalton Trans. 3584–3589 (2009)
51. Hennig, A., Ghale, G., Nau, W.M.: Effects of cucurbit[7]uril on enzymatic activity. Chem. Commun. 1614–1616 (2007)
52. Montes-Navajas, P., Gonzalez-Bejar, M., Scaiano, J.C., Garcia, H.: Cucurbituril complexes cross the cell membrane. Photochem. Photobiol. Sci. **8**, 1743–1747 (2009)
53. Kim, S.K., Park, K.M., Singha, K., Kim, J., Ahn, Y., Kim, K., Kim, W.J.: Galatosylated cucurbituril-inclusion polyplex for hepatocyte-targeted gene delivery. Chem. Commun. **46**, 692–694 (2010)
54. Lagona, J., Mukhopadhyay, P., Chakrabarti, S., Isaacs, L.: The Cucurbit[*n*]uril Family. Angew. Chem. Int. Ed. **44**, 4844–4870 (2005)
55. Bartulewicz, D., Bielawski, K., Bielawska, A.: Arch. Pharm. Pharm. Med. Chem. **9**, 422–426 (2002)
56. Lee, M., Rhodes, A.L., Wyatt, M.D., D'Incalci, M., Forrow, S., Hartley, J.A.: In vitro cytotoxicity ofGC sequence directed alkylating agents related to distamycin. J. Med. Chem. **36**, 863–870 (1993)
57. Becker, C., Dressman, J.B., Amidon, G.L., Junginger, H.E., Kopp, S., Midha, K.K., Shah, V.P., Stavchansky, S., Barends, D.M.: Biowaiver monographs for immediate release solid oral dosage forms: isoniazid. J. Pharm. Sci. **96**, 522–531 (2007)
58. Becker, C., Dressman, J.B., Amidon, G.L., Junginger, H.E., Kopp, S., Midha, K.K., Shah, V.P., Stavchansky, S., Barends, D.M.: Biowaiver monographs for immediate release solid oral dosage forms: pyrazinamide. J. Pharm. Sci. **97**, 3709–3720 (2008)
59. Zhou, Y., Yu, H., Zhang, L., Xu, H., Wu, L., Sun, J., Wang, L.: A new spectrofluorometric method for the determination of nicotine base on the inclusion interaction of methylene blue and cucurbit[7]uril. Microchim. Acta **164**, 63–68 (2009)
60. Takaki, Y., Sasada, Y., Watanabe, T.: The crystal structure of α-pyrazinamide. Acta Cryst. **13**, 693–702 (1960)
61. Rø, G., Sørum, H.: The crystal and molecular structure of δ-pyrazincarboxamide. Acta Cryst. **B28**, 1677–1684 (1972)
62. Tamura, C., Kuwano, H.: Crystallographic data of carboxylic acids and carboxyamides of picoline and pyrazine derivatives. Acta Cryst. **14**, 693 (1961)
63. Jensen, L.H.: The crystal structure of isonicotinic acid hydrazide. J. Am. Chem. Soc. **76**, 4663–4667 (1954)
64. Bhat, T.N., Singh, T.P., Vijayan, M.: Isonicotinic acid hydrazide—a reinvestigation. Acta Cryst. **B30**, 2921–2922 (1974)
65. Rastogi, R., Sultana, Y., Aqil, M., Kumar, S., Chuttani, K., Mishra, A.K.: Alginate microspheres of isoniazid for oral sustained drug delivery. Int. J. Pharm. **334**, 71–77 (2007)
66. Kim, J., Jung, I.-S., Kim, S.-Y., Lee, E., Kang, J.-K., Sakamoto, S., Yamaguchi, K., Kim, K.: New cucurbituril homologues: Syntheses, isolation, characterization, and X-ray crystal structures of cucurbit[*n*]uril ($n = 5$, 7, and 8). J. Am. Chem. Soc. **122**, 540–541 (2000)
67. Bhutani, H., Singh, S., Jindal, K.C.: Drug-drug interaction studies on first-line anti-tuberculosis drugs. Pharm. Dev. Technol. **10**, 517–524 (2005)
68. Brittain, H.G.: Polymorphism in Pharmaceutical Solids. Marcel Dekker Inc., New York (1999)
69. Day, A., Arnold, A.P., Blanch, R.J., Snushall, B.: Controlling factors in the synthesis of cucurbituril and its homologues. J. Org. Chem. **66**, 8094–8100 (2001)
70. Maple, J.R., Hwang, M.J., Stockfisch, T.P., Dinur, U., Waldman, M., Ewig, C.S., Hagler, A.T.: Derivation of class II force fields. I. Methodology and quantum force field for the alkyl functional group and alkane molecules. J. Comput. Chem. **15**, 162–182 (1994)
71. Chen, J., Brooks, C.L., Khandogin, J.: Recent advances in implicit solvent-based methods for biomolecular simulations. Curr. Opin. Struct. Biol. **18**, 140–148 (2008)
72. de Oliveira, A.M., Custodio, F.B., Donnici, C.L., Montanari, C.A.: Eur. J. Med. Chem. **38**, 141–155 (2003)